The Repetition Period of MeV Electron Microbursts as measured by SAMPEX/HILT

Hamdan Kandar[1], Lauren Blum[1,2], Mykhaylo Shumko[3], Lunjin Chen[4], Jih-Hong Shue[5]

[1]University of Colorado Boulder, Colorado, USA
[2]Laboratory for Atmospheric and Space Physics, Boulder, Colorado, USA
[3]The Johns Hopkins University Applied Physics Laboratory, Laurel, MD, USA
[4] University of Texas Dallas, Texas, USA
[5] Department of Space Science and engineering, National Central University, Jhongli, Taiwan

Corresponding author: Hamdan Kandar (Haka8022@colorado.edu)

Key Points:

- The repetition period of MeV electron microbursts is studied for the first time using 15 years of SAMPEX/HILT data
- Microburst repetition periods are most often <1 sec, and drop off as a power law moving to longer periods
- Repetition periods show strong agreement with chorus wave element periodicities in all MLT sectors except for the dusk sector

Abstract

Here we examine properties of MeV electron microbursts to better understand their generation mechanisms. Using 15 years of data from SAMPEX/HILT, >1MeV microburst repetition periods (time spacing between bursts) are examined and clear dependencies on AE, L shell, and MLT are discovered. Microburst repetition periods are shortest around 0-6 hr MLT and 4-5 Lshell, and grow longer towards the day and afternoon sectors and larger L shells. Shorter repetition periods (<1 sec) are also found to be more common during higher AE, while longer periods (>10 sec) more common during quiet times. The microburst repetition period distributions are compared directly to those of rising tone chorus wave elements and found to be similar in the night, dawn and day MLT sectors, suggesting chorus wave repetition periods are likely directly controlling those of microburst precipitation. However, dusk-side distributions differ, indicating that the dusk-side microbursts properties may be controlled by other processes.

Plain Language Summary

Looking at energetic electrons in Earth's magnetosphere from the HILT instrument on board the SAMPEX satellite helps us better understand the feature called microbursts. Microbursts are very rapid bursts of enhanced high-energy electrons entering our atmosphere. In this study, we characterize the properties of the microbursts to understand when, and where they happen, what causes them, and what impact they might have. We do so by looking at factors such as their magnetic local time as well as their time separation. This study also compares these microbursts' results to previous chorus wave studies. Chorus waves have been thought to be related to microbursts and could be a cause for some of their properties. We discuss more about this correlation in the result section of this study.

1 Introduction

Microbursts are rapid (sub-second) bursts of energetic electrons entering Earth's atmosphere from the magnetosphere. They have been shown to be a significant source of loss for the radiation belts during storm main and recovery phases (e.g. O'Brien et al. 2004, Thorne et al. 2005, Breneman et al. 2017, Blum et al. 2015), as well as a potential driver of mesospheric Ozone loss (Seppala et al. 2018, Duderstadt et al. 2021). Microbursts have been observed by numerous spacecraft in low Earth orbits, and can range from keV up to MeV energies (Elliott et al. 2022 and references within). Microbursts occur most frequently between 4 and 6 L shell and from midnight to morning (0 to 12 hr) magnetic local time (MLT) (Lorentzen et al. 2001, Nakamura et al. 2000). They typically last on the order of 100 ms, and estimates of the physical size of individual microbursts are on the order of 10 km (e.g. Shumko et al. 2021, Crew et al. 2016, Shumko et al. 2018, Shumko et al. 2020).

Due to their similar distributions in L shell and MLT, as well as their short sub-second durations, rising tone chorus waves have long been considered a primary mechanism for generating microbursts. Chorus waves have been shown to be able to resonate with energetic electrons, rapidly scattering them into the loss cone. Gyro-

resonant with keV electrons close to the magnetic equator, and as chorus wave packets propagate to higher magnetic latitudes they can resonate with higher energy (MeV) electrons (e.g. Horne and Thorne, 2003, Saito et al. 2012). Simulations as well as a handful of observations have shown a close correspondence between chorus waves in the magnetosphere and relativistic electron microbursts at low altitudes (e.g. Chen et al. 2022, Miyoshi et al. 2020, Breneman et al. 2017, Mozer et al. 2017).

Microbursts often occur in rapid succession, often refered to as microburst trains (e.g. O'Brien et al. 2004). It is still an open question what determines the time spacing (or repetition period) of trains of microbursts, as well as whether isolated microbursts are generated by the same mechanisms as trains. In this work, we explore the repetition period of MeV electron microbursts, to gain insight into the possible generation mechanisms for these repetition periods. Using 15 years of data from the Solar, Anomalous, Magnetospheric Particles Explorer (SAMPEX) satellite, we calculate the repetition period of MeV microbursts and examine its dependence on L shell, MLT, and AE. We then compare these patterns to those found in previous studies of chorus wave properties.

2 Methodology

2.1. Detecting microbursts

The Solar, Anomalous, Magnetospheric Particles Explorer (SAMPEX) satellite was designed to measure energetic nuclei and electrons over a broad dynamic range (Baker et al. 1993). SAMPEX was launched July 3 1992 into an 82 degree inclination orbit carrying four instruments. We use 20ms cadence measurements of >1 MeV electrons from the Heavy Ion Large Telescope (HILT) (Klecker et al. 1993) to detect relativistic electron microbursts from 1997 to 2012.

To detect microbursts in the SAMPEX/HILT data, we apply an algorithm developed by O'Brien et al. (2003) and applied in a number of previous studies:

$$(N_{100} - A_{500})/\sqrt{1 + A_{500}} > 10$$

where N is the number of counts in 100 ms and A_{500} is a running average over 500 ms. The threshold of the above ratio set to be 10 so that most microbursts are picked up while false detections are minimized. For each microburst time, if in the surrounding 250 HILT samples (nominally 5 seconds), there exists a data gap with duration exceeding 1 second, we discard that microburst detection, in order to remove false detections near data gaps. Applying this algorithm to the 15 years analyzed results in a total of 279,061 microburst detections. This database of microbursts detected by SAMPEX/HILT, while it was in State 4 (20 ms cadence) and while SAMPEX was not spinning, was compiled by and is available in Shumko et al. 2021.

2.2. Calculating the repetition period

Once we have the list of microburst detections with assigned date and time, we then calculate the time between each microburst (denoted as dt). Figure 1a shows the application of the O'Brien et al. (2003) microburst detection algorithm as applied to SAMPEX data, as well as how the repetition period (dt) is estimated. Figure 1b shows the overall distribution of dt's during the 15 year period analyzed. We see from this that most microbursts occur less than one second apart. The number of microbursts drops off as a power law when moving to larger time separations, with slope ~ 0.46.

a)

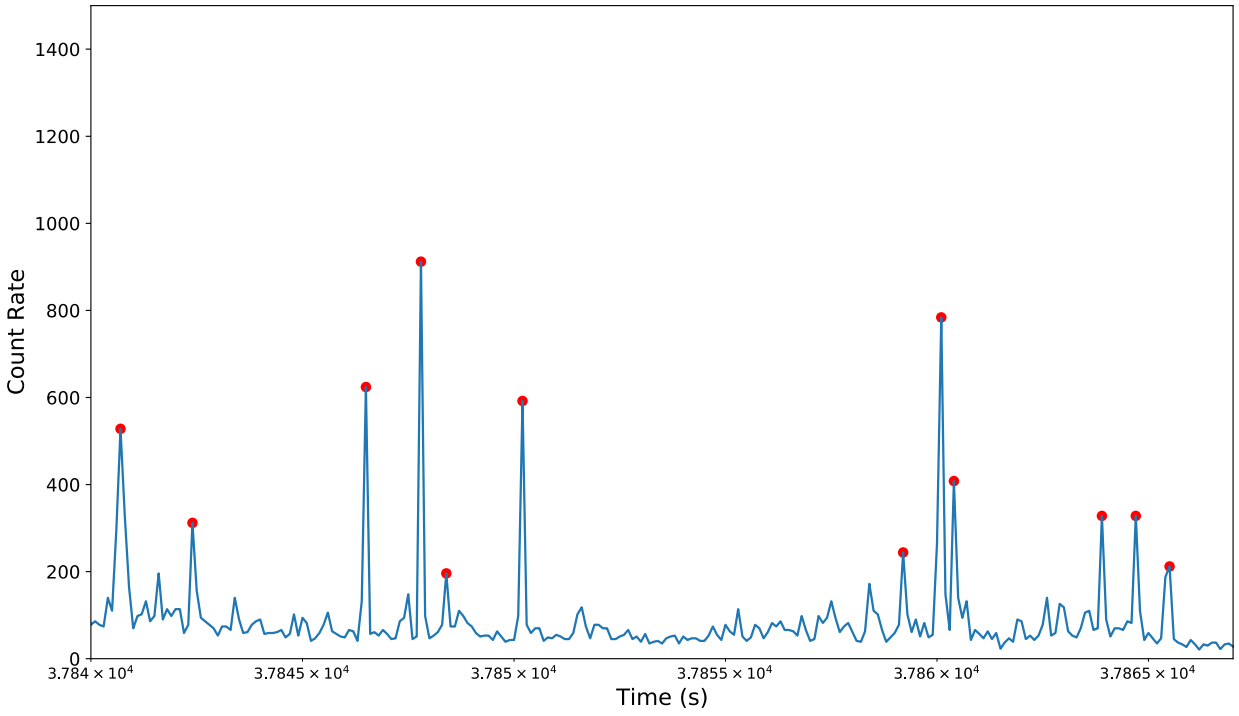

b)

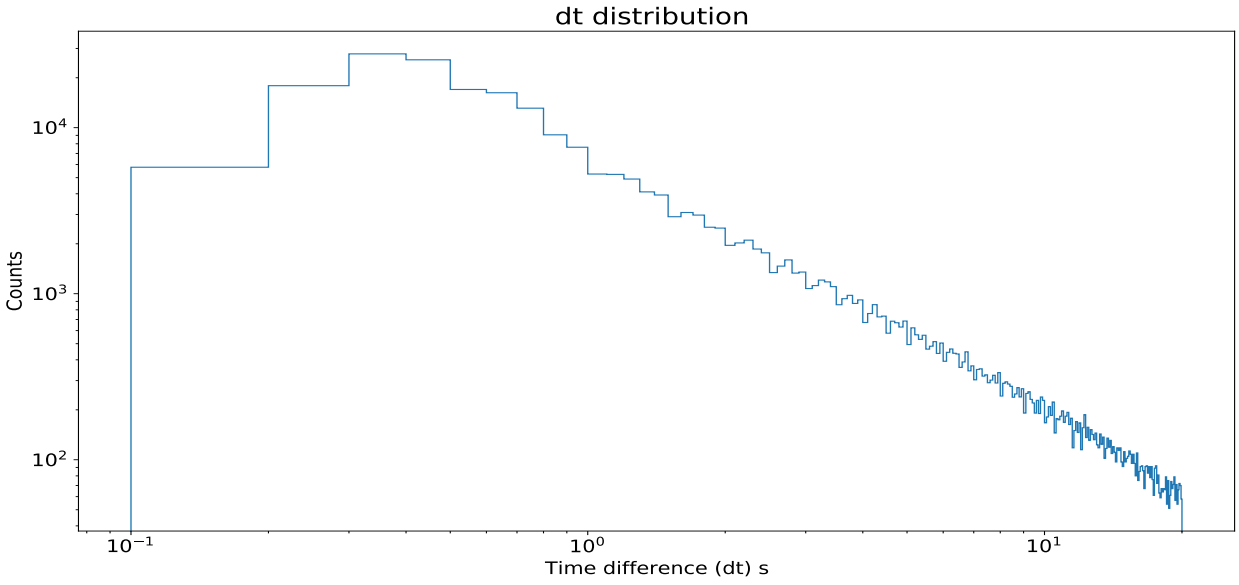

Figure 1. a) Count rates from SAMPEX HILT (blue) with microbursts detected by the O'Brien et al. (2003) algorithm (red). The space between the microburst detections represents the repetition period (dt). b) Distribution of the time difference between neighboring microbursts in seconds, with both axes on a log scale. Most microbursts occur less than one second apart.

3 Results

3.1. L shell and MLT dependence

With the large database of microbursts and their time separations (dt's) produced in the steps above, we now explore how the distribution of dt varies with location and geomagnetic activity.

Figure 2a shows the distribution of overall microburst in MLT and L shell. The number of microburst detections are binned into 1 L by 1 MLT bins. Microbursts are most frequent on the morning side of the magnetosphere, from ~4-6 L shell, in good agreement with past studies (O'Brien et al. 2003). This figure also shows that even in the afternoon sector, more than ~100 detections go into bins from 4-6 L shell, providing sufficient statistics for examining microburst repetition periods away from their location of peak occurrence as well.

Figure 2b shows the median dt in each MLT-L shell bin. Bins with less than 10 microbursts are white. A clear pattern is evident here, with closely spaced microbursts located primarily in the dawn sector and at low L shells, while microbursts further separated in time occur primarily after 12 MLT. The repetition period grows longer as one moves around in MLT from midnight to noon and to larger L shells. Isolated microbursts, with unusually longer dt ~ 10 seconds, are often observed at L~6 in the afternoon sector.

a) **b)**

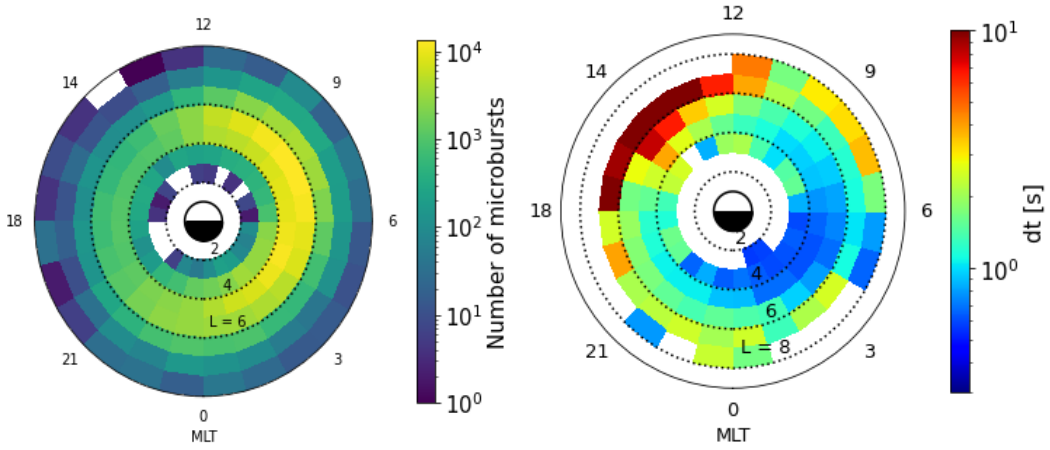

Figure 2. a) Distribution of microbursts in L shell and MLT. b) Distribution of the median dt in each MLT and L shell bin. Bins with less than 10 microbursts are white.

3.2. AE dependence

Next, we look at the dependencies of dt on geomagnetic activity, specifically the Auroral Electrojet (AE) index. Here we sort the microbursts into three categories – those occurring within 1 second of another microburst, those between 1 and 10 seconds of another microburst, and those >10 seconds from other microbursts. Figure 3 shows the microburst repetition period probability density function (PDF) in each of those AE categories. The width of the AE bins is set to be 50 nT.

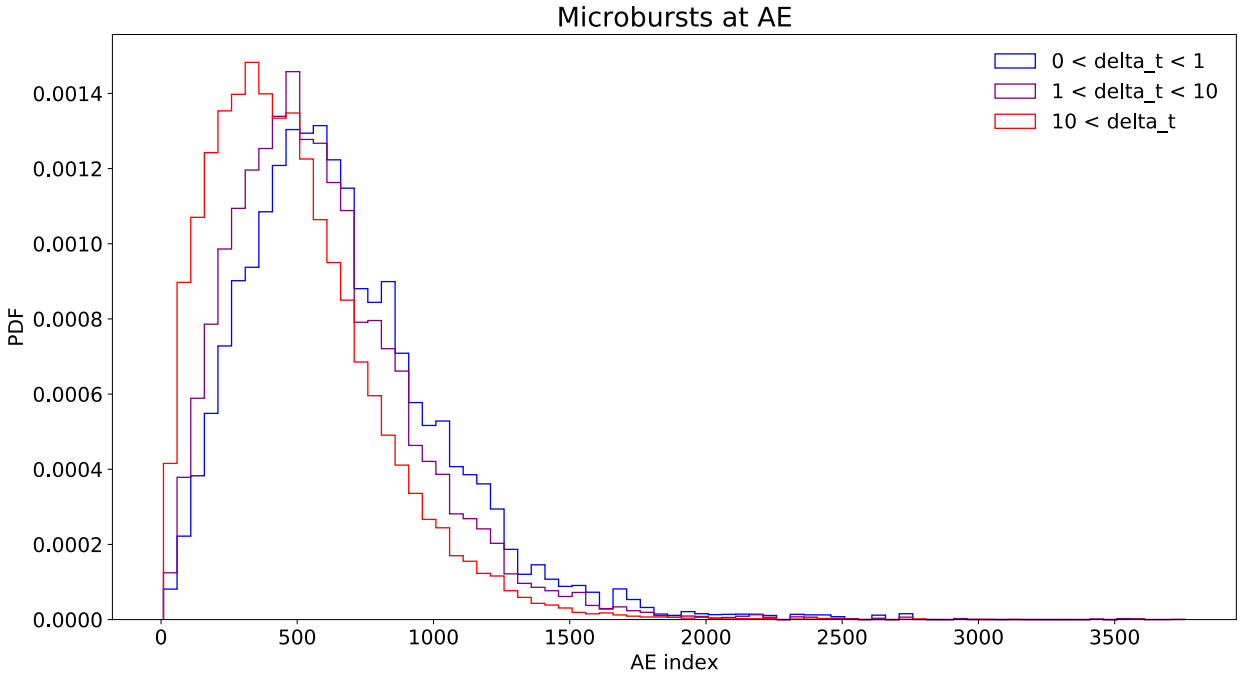

Figure 3. Normalized distributuion of the number of microbursts vs AE index in three different dt categories. For the dt < 1 second (Blue) the distribution peaks at a value of 559 nT in AE. For 1 < dt < 10s (purple) the peak is at 459 nT in AE. Finally for dt > 10 seconds (red) the peak is 309 nT in AE.

The results from Figure 3 reveal that microburst repetition period has an AE dependency as well. We see that for the dt category of > 10 seconds (red) the curve peaks at 309 nT in AE, while for the dt category of < 1 second (blue) the curve peaks at 559 nT in AE. Thus, during active times, when AE is larger, closely spaced microbursts are more prevalent, while occurrences of more isolated microbursts peak during lower AE values.

4 Discussion

The results above show clear dependencies of microburst repetition period on MLT, L shell, and AE. To better understand potential causes of these trends in the microburst repetition period, we compare to past studies of this similar repetition period property for chorus waves.

Shue et al. (2015) and Gao et al. (2022) have explored the dependence of rising tone chorus element repetition periods on MLT and both studies found a strong dependence similar to that shown here. Chorus wave repetition periods were shortest in the night and dawn sectors, and longer on the day and duskside. Background magnetic field strength and electron temperature were found to be controlling factors for this chorus repetition period (Shue et al. 2015). Gao et al. (2022) observed an inverse correlation between chorus repetition period and the drift velocity of electrons, suggesting faster drifting electrons produce more rapidly repeating chorus wave elements. Thus the electron refilling rate in a given region, from freshly injected particles on the nightside, directly controls chorus element density (or repetition periods).

Figure 4 shows probability distribution function of microburst dt's (blue) overlaid with that of chorus waves as derived from Shue et al. (2015) (orange) for the four different MLT sectors. We find very close agreement between these microburst and chorus wave distributions in the night (21-3 hr), dawn (03-09 hr), and day (09-15 hr) MLT sectors, suggesting chorus wave repetition periods are likely directly controlling those of microburst precipitation. This similarity between chorus wave and microburst properties also likely explains the AE dependences found in Figure 3. The refilling rate of freshly injected electrons on the nightside, which provide the free energy for chorus wave generation, is higher during more active geomagnetic conditions, thus resulting in higher repetition period microbursts as compared to quiet times.

Interestingly, we find that the distributions on the duskside (15-21 hr in MLT) do not show the same agreement, indicating that the dusk side microbursts properties may be controlled by processes other than interaction with chorus wave. Meyer-Reed et al. (2023), looking at the pitch angle anisotropy of microbursts rather than repetition period, also found that duskside microburst properties differed from those in other local time sectors. There have also been a few case studies suggesting EMIC waves, rather than chorus waves, may be a possible source of MeV electron microbursts in the dusk sector (e.g. Shumko et al. 2022, Douma et al. 2017). Further investigation into the drivers of dusk-side MeV electron microburst precipitation is needed to better understand the difference demonstrated in Figure 4 between the precipitation properties and those of chorus waves.

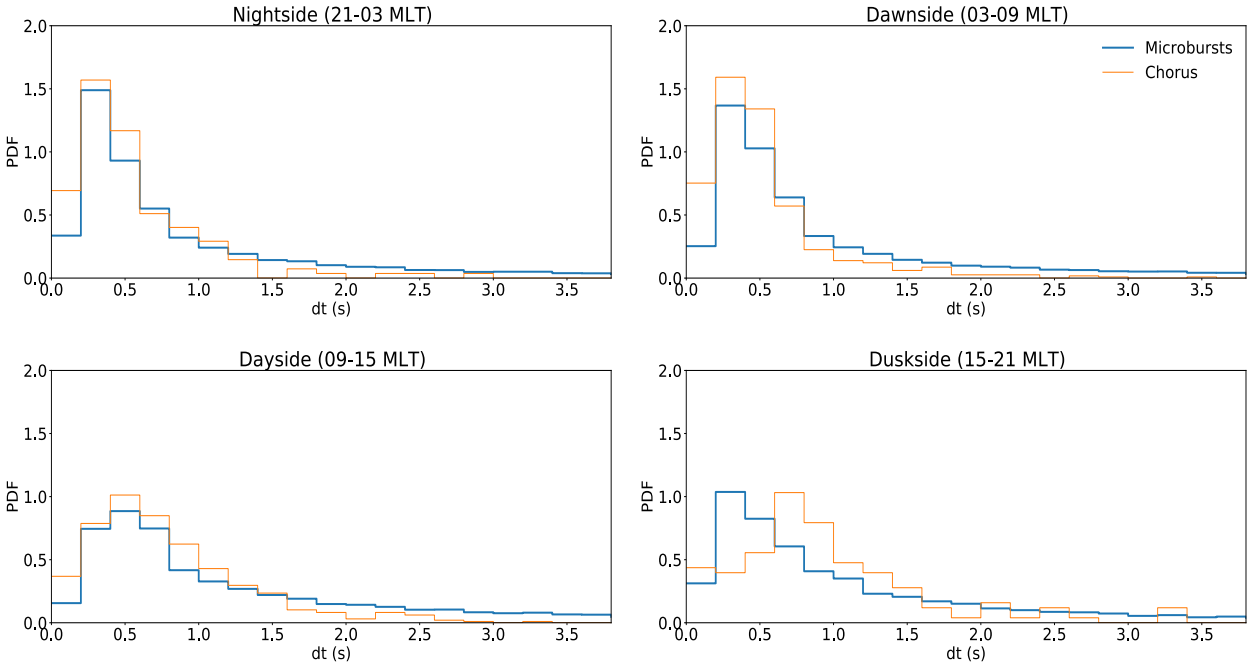

Figure 4. Distributions of the chorus wave (orange) and microbursts (blue) repetition periods in four different MLT categories. Chorus wave distributions are taken from Shue et al. (2015).

5 Summary

Here we examine 15 years of SAMPEX data to better understand the detailed properties of MeV electron microbursts, particularly their repetition periods, for the first time. We find:

1. Microburst repetition periods are most often <1 sec, the distribution follows a decaying power law.
2. Repetition periods show clear dependencies on MLT, L shell, and AE. The periods peaks near noon and L=4-6, and tend to be shorter for higher AE.
3. The distribution of microburst dt's shows very strong agreement with that of chorus wave rising tone elements in the night, dawn, and day-side MLT sectors, while dusk-side distributions do not match well.

These findings illustrate the insight to be gained from exploring the detailed properties of MeV electron microbursts. The repetition period distributions found here highlight the close connection between chorus wave properties and MeV microburst properties on the night, dawn, and day-sides of the magnetosphere, and provide insight into the magnetospheric conditions controlling the trains of microburst precipitation often observed. These findings also reveal the unusual repetition periods of dusk-sector microbursts, suggesting potentially different generation mechanisms or plasma properties mediating the wave-particle interactions in this sector play a role.

Acknowledgments

This work was supported in part by NASA's H-SR award #80NSSC21K1682, as well as the NASA/Goddard ISFM Space Precipitation Impacts (SPI) team, grant HISFM21. LC acknowledges the support of NASA grant 80NSSC21K1320**.**

Open Research

The sampex data center at Caltech has provided the data which is accessible to the public. Retrieved from https://izw1.caltech.edu/sampex/DataCenter/index.html The catalog of SAMPEX/HILT microbursts, and the analysis software used here, is available at: **https://github.com/mshumko/sampex_microburst_widths**, and is archived on Zenodo **https://doi.org/10.5281/zenodo.5165064**.

References

Baker, D. N., Mason, G. M., Figueroa, O., Colon, G., Watzin, J. G., & Aleman, R. M. (1993). An overview of the solar anomalous, and Magnetospheric Particle Explorer (SAMPEX) mission. *IEEE Transactions on Geoscience and Remote Sensing*, *31*(3), 531–541. https://doi.org/10.1109/36.225519

Blum, L., Li, X., & Denton, M. (2015). Rapid Mev electron precipitation as observed by Sampex/hilt during high-speed stream-driven storms. *Journal of Geophysical Research: Space Physics*, *120*(5), 3783–3794. https://doi.org/10.1002/2014ja020633

Blum, L. W., and Breneman, A. W. (2020). "Chapter 3—observations of radiation belt losses due to cyclotron wave-particle interactions ''in The dynamic loss of Earth's radiation belts. Tharamani, Chennai: Elsevier. doi:10.1016/B978-0-12-813371-2.00003-2

Breneman, A. W., Crew, A., Sample, J., Klumpar, D., Johnson, A., Agapitov, O., Shumko, M., Turner, D. L., Santolik, O., Wygant, J. R., Cattell, C. A., Thaller, S., Blake, B., Spence, H., & Kletzing, C. A. (2017). Observations directly linking relativistic electron microbursts to Whistler Mode Chorus: Van allen probes and Firebird II. *Geophysical Research Letters*, *44*(22). https://doi.org/10.1002/2017gl075001

Chen, L., Zhang, X. J., Artemyev, A., Angelopoulos, V., Tsai, E., Wilkins, C., & Horne, R. B. (2022). Ducted Chorus waves cause sub-relativistic and relativistic electron microbursts. *Geophysical Research Letters*, *49*(5). https://doi.org/10.1029/2021gl097559

Crew, A. B., Spence, H. E., Blake, J. B., Klumpar, D. M., Larsen, B. A., O'Brien, T. P., et al. (2016). First multipoint *in situ* observations of electron microbursts: Initial results from the NSF

FIREBIRD II mission. *J. Geophys. Res. Space Phys.* 121 (6), 5272–5283. doi:10.1002/2016ja022485

Douma, E., Rodger, C. J., Blum, L. W., & Clilverd, M. A. (2017). Occurrence characteristics of relativistic electron microbursts from Sampex observations. *Journal of Geophysical Research: Space Physics*, *122*(8), 8096–8107. https://doi.org/10.1002/2017ja024067

Duderstadt, K. A., Huang, C. -L., Spence, H. E., Smith, S., Blake, J. B., Crew, A. B., Johnson, A. T., Klumpar, D. M., Marsh, D. R., Sample, J. G., Shumko, M., & Vitt, F. M. (2021). Estimating the impacts of radiation belt electrons on atmospheric chemistry using Firebird II and Van Allen probes observations. *Journal of Geophysical Research: Atmospheres*, *126*(7). https://doi.org/10.1029/2020jd033098

Elliott, S. S., Breneman, A., Colpitts, C., Bortnik, J., Jaynes, A., Halford, A., Shumko, M., Blum, L., Chen, L., Greeley, A., & Turner, D. (2022). Understanding the properties, wave drivers, and impacts of electron microburst precipitation: Current understanding and critical knowledge gaps. *Frontiers in Astronomy and Space Sciences*, *9*. https://doi.org/10.3389/fspas.2022.1062422

Gao, X., Chen, R., Lu, Q., Chen, L., Chen, H., & Wang, X. (2022). Observational evidence for the origin of repetitive chorus emissions. *Geophysical Research Letters*, *49*(12). https://doi.org/10.1029/2022gl099000

Horne, R. B., & Thorne, R. M. (2003). Relativistic electron acceleration and precipitation during resonant interactions with Whistler-Mode Chorus. *Geophysical Research Letters*, *30*(10). https://doi.org/10.1029/2003gl016973

Klecker, B., Hovestadt, D., Scholer, M., Arbinger, H., Ertl, M., Kastele, H., Kunneth, E., Laeverenz, P., Seidenschwang, E., Blake, J. B., Katz, N., & Mabry, D. (1993). Hilt: A heavy ion large area proportional counter telescope for solar and Anomalous Cosmic Rays. *IEEE Transactions on Geoscience and Remote Sensing*, *31*(3), 542–548. https://doi.org/10.1109/36.225520

Kurita, S., Miyoshi, Y., Blake, J. B., Reeves, G. D., & Kletzing, C. A. (2016). Relativistic electron microbursts and variations in trapped MeV electron fluxes during the 8–9 October 2012 storm: Sampex and van allen probes observations. *Geophysical Research Letters*, *43*(7), 3017–3025. https://doi.org/10.1002/2016gl068260

Lorentzen, K. R., Looper, M. D., & Blake, J. B. (2001). Relativistic electron microbursts during the gem storms. *Geophysical Research Letters*, *28*(13), 2573–2576. https://doi.org/10.1029/2001gl012926

Meyer-Reed, C., Blum, L., & Shumko, M. (2023). Pitch angle isotropy of relativistic electron microbursts as observed by SAMPEX/Hilt: Statistical and storm-time properties. *Journal of Geophysical Research: Space Physics*, *128*(1). https://doi.org/10.1029/2022ja030926

312 Miyoshi, Y., Saito, S., Kurita, S., Asamura, K., Hosokawa, K., Sakanoi, T., Mitani, T., Ogawa,
313 Y., Oyama, S., Tsuchiya, F., Jones, S. L., Jaynes, A. N., & Blake, J. B. (2020). Relativistic
314 electron microbursts as high-energy tail of pulsating Aurora electrons. *Geophysical*
315 *Research Letters*, *47*(21). https://doi.org/10.1029/2020gl090360

316 Mozer, F. S., Agapitov, O. V., Blake, J. B., & Vasko, I. Y. (2018). Simultaneous observations of
317 lower band chorus emissions at the equator and microburst precipitating electrons in the
318 ionosphere. *Geophysical Research Letters*, *45*(2), 511–516.
319 https://doi.org/10.1002/2017gl076120

320 Nakamura, R., Isowa, M., Kamide, Y., Baker, D. N., Blake, J. B., and Looper, M. (2000).
321 SAMPEX observations of precipitation bursts in the outer radiation belt. *J. Geophys. Res.* 105
322 (A7), 15875–15885. doi:10.1029/2000JA900018

323 O'Brien, T. P. (2003). Energization of relativistic electrons in the presence of Ulf Power and
324 MeV microbursts: Evidence for dual ulf and VLF acceleration. *Journal of Geophysical*
325 *Research*, *108*(A8). https://doi.org/10.1029/2002ja009784

326 O'Brien, T. P., Looper, M. D., and Blake, J. B. (2004). Quantification of relativistic electron
327 microburst losses during the GEM storms. *Geophys. Res. Lett.* 31, L04802.
328 doi:10.1029/2003GL018621
329
330 Seppälä, A., Douma, E., Rodger, C., Verronen, P., Clilverd, M. A., and Bortnik, J. (2018).
331 Relativistic electron microburst events: Modeling the atmospheric impact. *Geophys. Res.*
332 *Lett.* 45, 1141–1147. doi:10.1002/2017GL075949

333 Shue, J. H., Hsieh, Y. K., Tam, S. W., Wang, K., Fu, H. S., Bortnik, J., Tao, X., Hsieh, W. C., &
334 Pi, G. (2015). Local time distributions of repetition periods for rising tone lower band
335 chorus waves in the magnetosphere. *Geophysical Research Letters*, *42*(20), 8294–8301.
336 https://doi.org/10.1002/2015gl066107

337 Shumko, M., Blum, L. W., & Crew, A. B. (2021). Duration of individual relativistic electron
338 microbursts: A probe into their scattering mechanism. *Geophysical Research Letters*,
339 *48*(17). https://doi.org/10.1029/2021gl093879

340 Shumko, M., Sample, J., Johnson, A., Blake, B., Crew, A., Spence, H., Klumpar, D., Agapitov,
341 O., & Handley, M. (2018). Microburst scale size derived from multiple bounces of a
342 microburst simultaneously observed with the Firebird-II CubeSats. *Geophysical Research*
343 *Letters*, *45*(17), 8811–8818. https://doi.org/10.1029/2018gl078925

344 Shumko, M., Gallardo-Lacourt, B., Halford, A. J., Blum, L. W., Liang, J., Miyoshi, Y.,
345 Hosokawa, K., Donovan, E., Mann, I. R., Murphy, K., Spanswick, E. L., Blake, J. B.,
346 Looper, M. D., & Gillies, D. M. (2022). Proton Aurora and relativistic electron microbursts
347 scattered by electromagnetic ion cyclotron waves. *Frontiers in Astronomy and Space*
348 *Sciences*, *9*. https://doi.org/10.3389/fspas.2022.975123

Shumko, M., Johnson, A. T., Sample, J. G., Griffith, B. A., Turner, D. L., O'Brien, T. P., Agapitov, O., Blake, J. B., & Claudepierre, S. G. (2020). Electron microburst size distribution derived with AeroCube-6. *Journal of Geophysical Research: Space Physics*, *125*(3). https://doi.org/10.1029/2019ja027651

Saito, S., Y. Miyoshi, and K. Seki (2012), Relativistic electron microbursts associated with whistler chorus rising tone elements: GEMSIS-RBW simulations, J. Geophys. Res., 117, A10206, doi:10.1029/2012JA018020.

Thorne, R. M., O'Brien, T. P., Shprits, Y. Y., Summers, D., and Horne, R. B. (2005). Timescale for MeV electron microburst loss during geomagnetic storms. *J. Geophys. Res.* 110, A09202. doi:10.1029/2004JA010882